Supplemental Figure 1

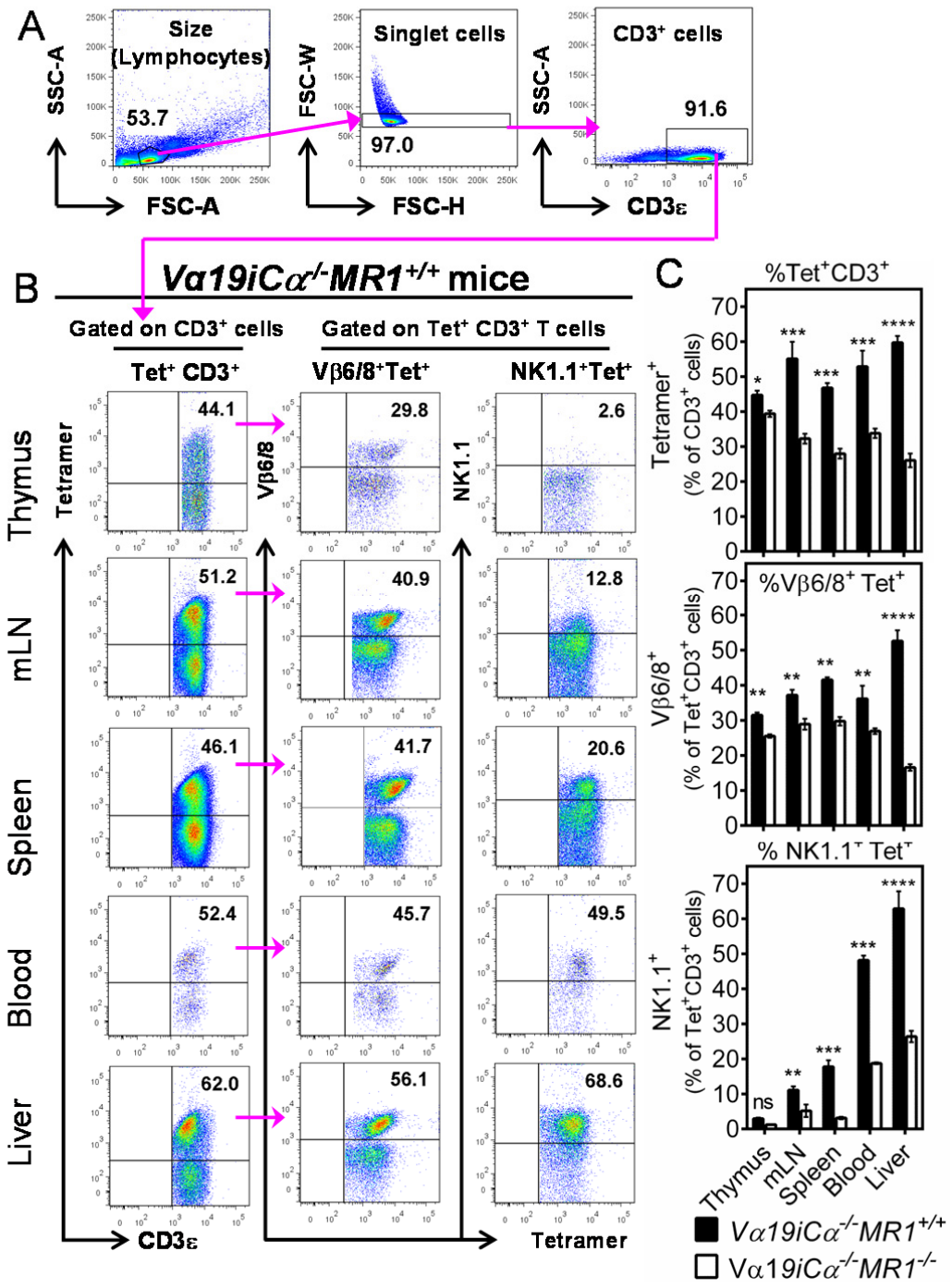

Supplemental Figure 1: **Frequency and Vβ6/8, NK1.1 phenotype of tetramer$^+$ CD3$^+$ T cells in the thymus, secondary lymphoid organs and peripheral sites.** (**A**). Gating strategy of SSC-A vs. FSC-A to define lymphocyte population, FSC-W vs. FSC-H for doublet

discrimination and SSC-A vs. CD3ε for $CD3^+$ T cells. (**B**) Representative FACS plots of $tetramer^+$ $CD3^+$ T cells (*left dot plots column*), $tetramer^+$ $V\beta6/8^+$ (*middle dot plots column*) and $tetramer^+$ $NK1.1^+$ (right dot plots column) cells in the thymus ($CD3^{high}$, mature thymocytes), mesenteric lymph nodes (mLN), spleen, blood and liver from $V\alpha19iC\alpha^{-/-}MR1^{+/+}$ mice. Numbers in the upper right quadrants are proportions of $CD3^+$ cells that were $tetramer^+$ (left column) and $tetramer^+$ $CD3^+$ T cells that expressed Vβ6/8 (middle column) and NK1.1 (right column). (**C**) Shown are bar graphs of proportions of $tetramer^+$ $CD3^+$ T cells (top panel), $V\beta6/8^+$ $tetramer^+$ $CD3^+$ T cells (middle panel) and $NK1.1^+$ $tetramer^+$ $CD3^+$ T cells (bottom panel). Data shown are from more than three experiments. *P values* (obtained by 2way ANOVA, multiple comparison test) denote comparison between $V\alpha19iC\alpha^{-/-}MR1^{+/+}$ (filled bars) and $V\alpha19iC\alpha^{-/-}MR1^{-/-}$ (open bars). $*p<0.05$; $**p<0.01$, $***p<0.001$ and $***p<0.0001$.

Supplemental Figure 2

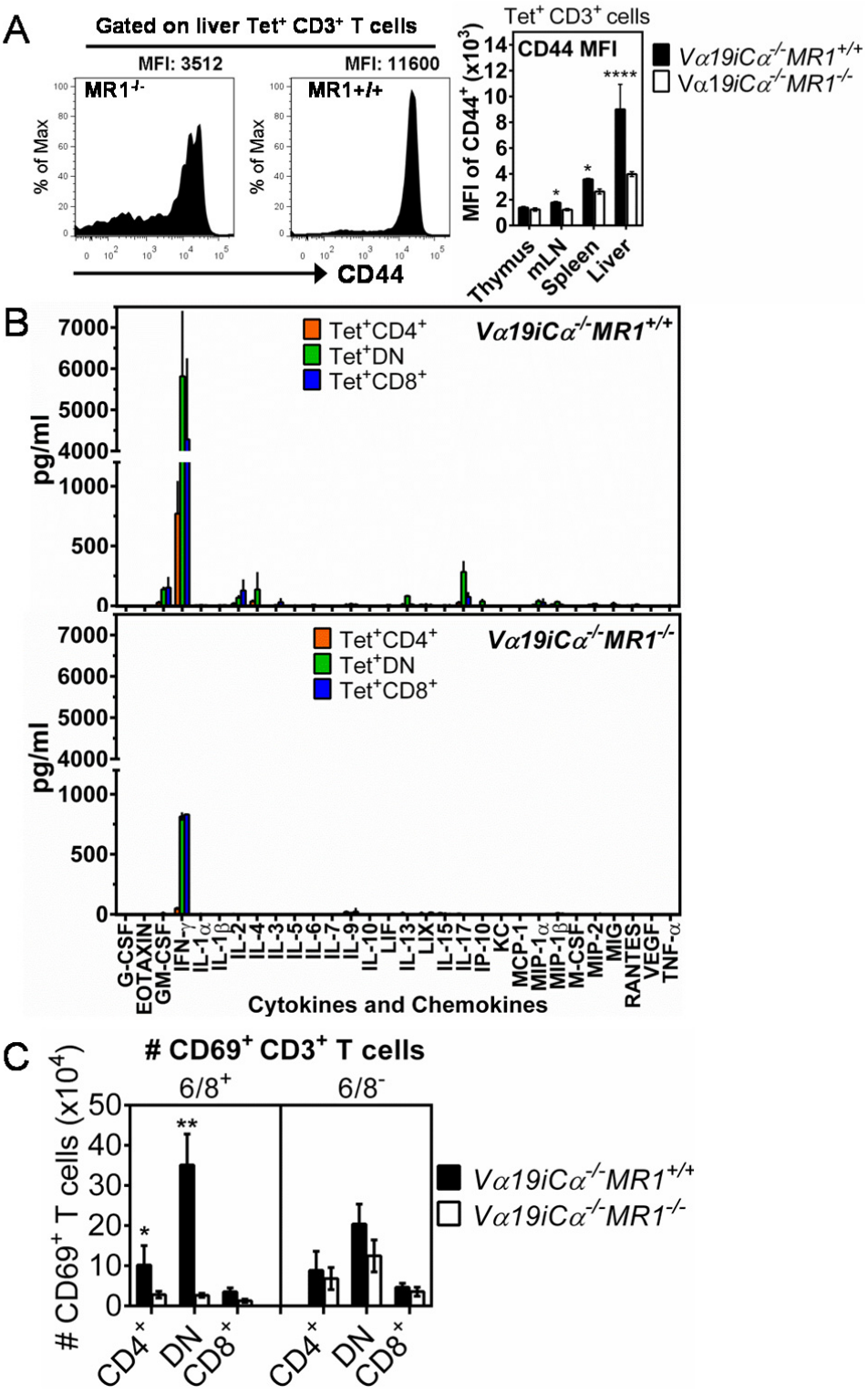

Supplemental Figure 2: (**A**) CD44 staining in tetramer^{+} CD3^{+} T cells in the thymus, secondary lymphoid organs (mLN and spleen) and peripheral cells (liver). (**B**) *Vα19iCα$^{-/-}$*

MR1$^{+/+}$ T cells respond to IL-12 plus IL-18 better than *Vα19iTgMR1*$^{-/-}$ T cells. Purified splenic T cells from *Vα19iCα*$^{-/-}$*MR1*$^{+/+}$ (top panel) or *Vα19iCα*$^{-/-}$*MR1*$^{-/-}$ (bottom panel) mice were stained with antibodies specific for CD3ε, CD4, CD8α and MR1/RL tetramer, and tetramer^{+} cells sorted by FACS. Sorted tetramer^{+} T cells were rested overnight in medium and then cultured (2 x 10^5 cells/well) in triplicates with 500 pg/ml IL-12 plus 1000 pg/ml IL-18 in the absence of APC for 24h at 37°C. The indicated cytokines and chemokines were measured in supernatants using Multiplex bead array assays according to manufacturer's instructions (Milliplex MAP Assays from EMD Millipore). Tetramer^{+} *Vα19iCα*$^{-/-}$*MR1*$^{+/+}$ T cells (DN/CD8^{+} > CD4^{+}) produced more IFN-γ than their counterparts that developed in the absence of MR1. (C) Absolute numbers of Vβ6/8$^{+/-}$ CD69^{+} CD3^{+} T cells in the spleen of *Vα19iCα*$^{-/-}$*MR1*$^{+/+}$ vs. *Vα19iCα*$^{-/-}$*MR1*$^{-/-}$ mice. Data shown are from two separate experiments. *P* values were obtained by Mann-Whitney U-test and 2way ANOVA (multiple comparison test) (*p<0.05, ***p*<0.01 and ****p<0.0001).

Supplemental Figure 3

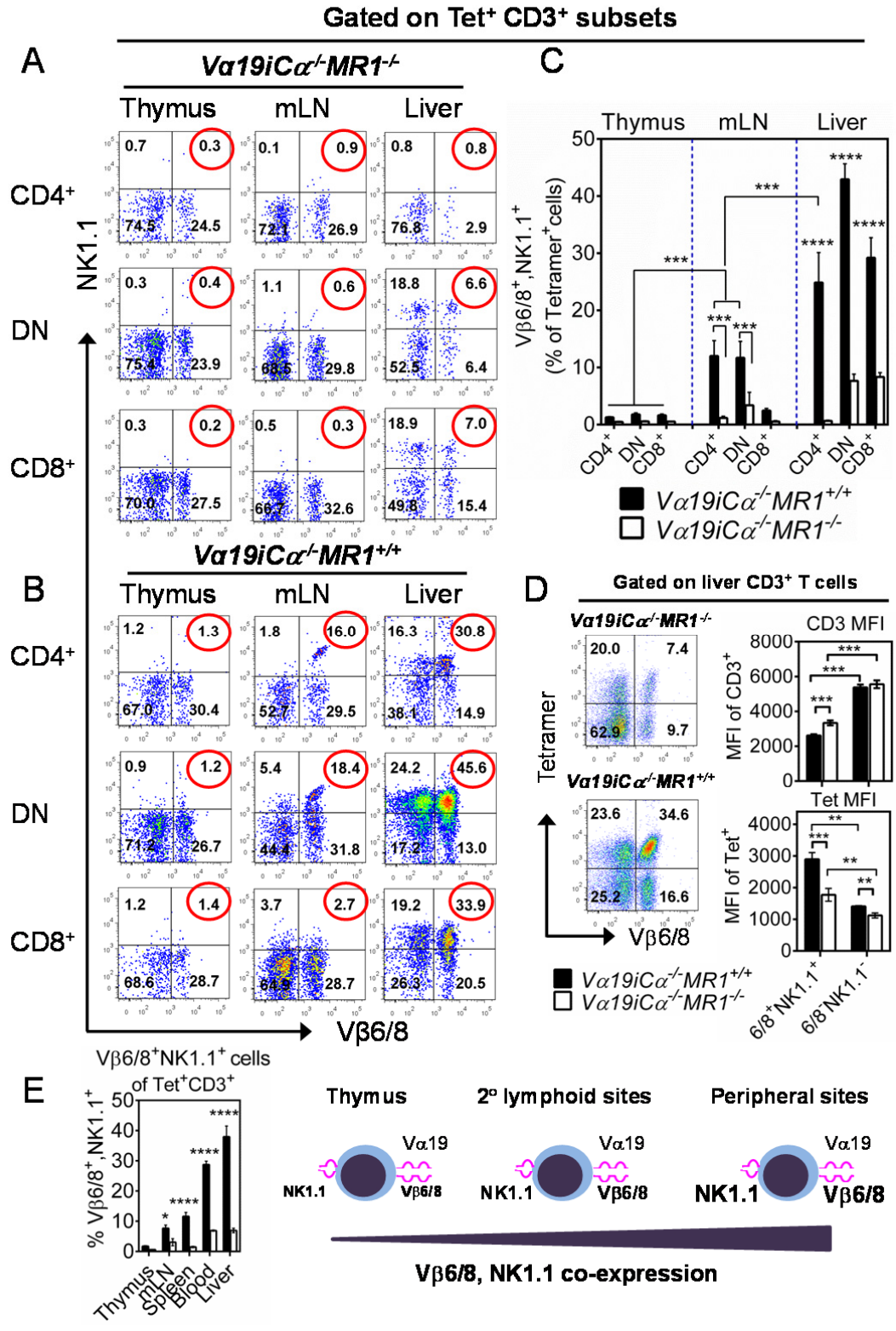

Supplemental Figure 3: Gradual increase in frequency of tetramer$^+$ CD3$^+$ cell subsets co-expressing Vβ6/8 and NK1.1 comparing mature thymocytes with secondary lymphoid

organs and peripheral sites. (**A and B**) Shows surface Vβ6/8.1-2 (X-axis) and NK1.1 (Y-axis) expression on tetramer$^+$ CD4$^+$ (*top dot plots*), DN (*middle dot plots*) or CD8$^+$ (*bottom dot plots*) in thymus, mesenteric lymph nodes, (mLN) and liver in uninfected *Vα19iCα*$^{-/-}$*MR1*$^{-/-}$ (A) *Vα19iCα*$^{-/-}$*MR1*$^{+/+}$ (B) mice. Numbers in the upper right quadrants are Vβ6/8.1-2$^+$ and NK1.1$^+$ cells. (**C**) Increasing proportions of Vβ6/8$^+$ and NK1.1$^+$ tetramer$^+$ CD3$^+$ T cell subsets from thymus (CD3^{high}, mature thymocytes; n=9), mLN (n=5) and Liver (n=4). (**D**) *Vα19i* Tg cells developing with MR1 have higher affinity for MR1/RL complexes. Shown in the left panel are Vβ6/8 (X-axis) vs. tetramer (Y-axis) FACS plots of CD3$^+$ T cells in liver from *Vα19iCα*$^{-/-}$*MR1*$^{-/-}$or *Vα19iCα*$^{-/-}$*MR1*$^{+/+}$ mice. Shown in the right panel are mean fluorescence intensities of CD3ε (top bar graph) and tetramer (bottom bar graph) staining on liver tetramer$^+$ Vβ6/8$^+$NK1.1$^+$ or Vβ6/8$^-$NK1.1$^-$ CD3$^+$ T cells from *Vα19iCα*$^{-/-}$*MR1*$^{+/+}$ or *Vα19iCα*$^{-/-}$*MR1*$^{-/-}$ mice (n=4). Despite lower CD3 expression, *Vα19i* Tg T cells from MR1$^{+/+}$ mice display higher affinity for MR1/RL tetramers than *Vα19i* Tg cells from MR1$^{-/-}$ mice. Furthermore, tetramer$^+$ CD3$^+$ T cells expressing both Vβ6/8 and NK1.1 in *Vα19i* Tg MR1 sufficient mice display the highest affinity for tetramer binding. (**E**) Bar graph showing composite proportions of Vβ6/8$^+$, NK1.1$^+$ among tetramer$^+$ CD3$^+$ T cells from MR1$^{+/+}$ (filled bars) and MR1$^{-/-}$ (open bars) mice and a summary illustration of progressive increases in Vβ6/8, NK1.1 co-expression on tetramer$^+$ MAIT cells with peripheral activation. *P* values were obtained by Mann-Whitney U-test and 2way ANOVA (multiple comparison test) (*p<0.05, **p<0.01, ***p<0.001 and ****p<0.0001).

Supplemental Figure 4

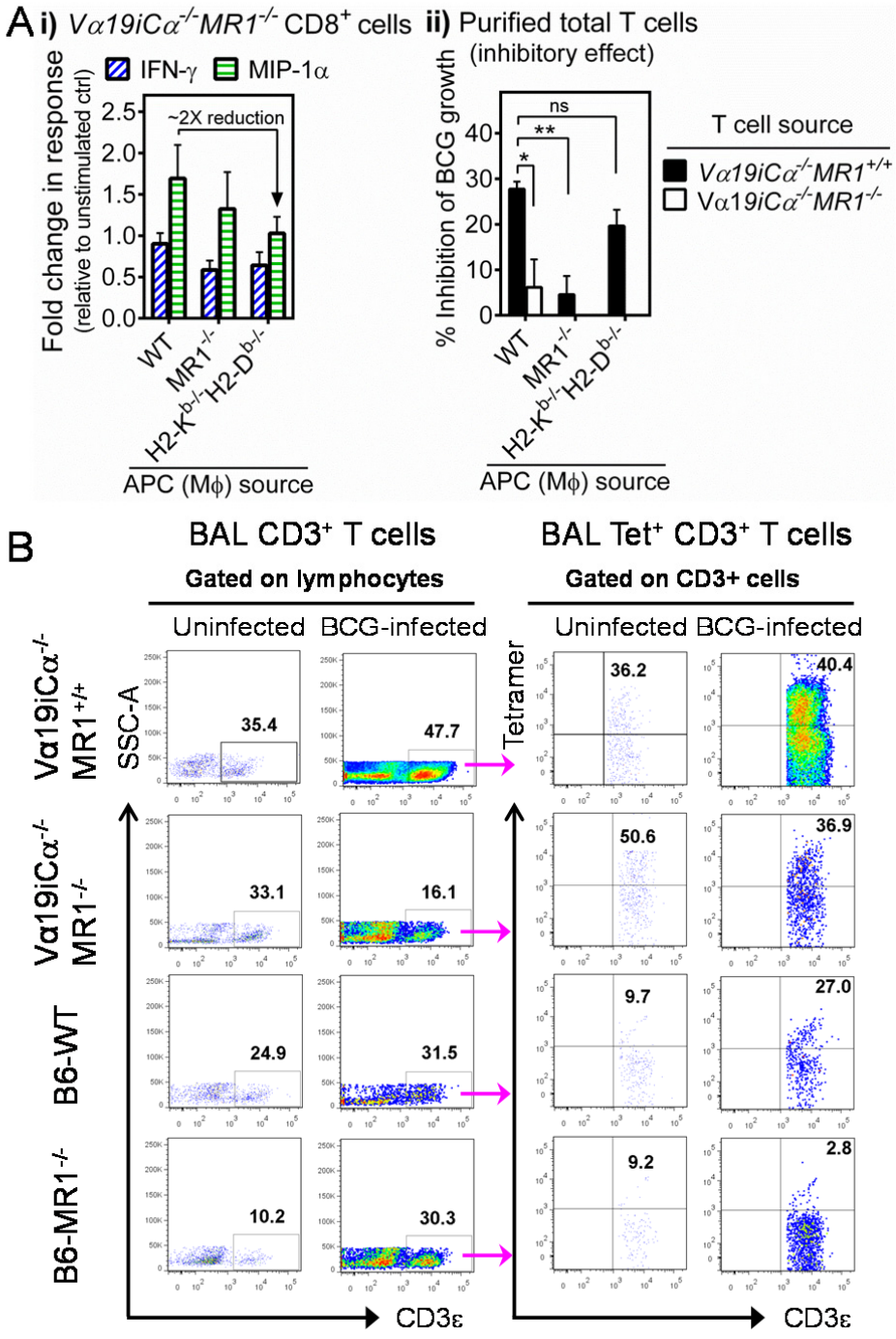

Supplemental Figure 4: (**A**) Evidence that *Vα19iCα*$^{-/-}$*MR1*$^{-/-}$ T cells interact with MHC class 1a molecules. (**A-i**) Purified *Vα19iCα*$^{-/-}$*MR1*$^{-/-}$ CD8^{+} T cells from three individual mice were co-cultured for 24h at 37ºC with uninfected or BCG Danish-infected BMDMϕ from B6-WT, B6-MR1$^{-/-}$ and H2-K$^{b-/-}$/H2-D$^{b-/-}$ mice. Activation of CD8^{+} T cells was determined by

intracellular cytokine staining for IFN-γ and MIP-1α/CCL3 using flow cytometry. Shown are relative fold increases in $CD8^+$ T cell IFN-γ and MIP-1α/CCL3 responses. There were approximately 2-fold reductions in MIP-1α//CCL3 responses when $CD8^+$ T cells were co-cultured with $H2\text{-}K^b/H2\text{-}D^b$ double knockout APC, indicating recognition of epitopes presented by MHC class Ia molecules. (**A-ii**) Inhibition of intracellular mycobacteria growth by purified total T cells from *Vα19iCα*$^{-/-}$*MR1*$^{-/-}$ mice was reduced in MR1 or MHC class Ia deficient macrophages, indicating a role for both MR1 and MHC class 1a molecules in the activation and function of *Vα19i* Tg T cells developing in the absence of MR1. (**B**) Representative FACS plots of CD3ε (X-axis) vs. SSC-A (Y-axis) gated on lymphocyte population for $CD3^+$ T cells (left panel of dot plots) and CD3ε (X-axis) vs MR1−5-OP-RU tetramer (Y-axis) gated on $CD3^+$ lymphocyte population for $tetramer^+$ $CD3^+$ T cells (right panel of dot plots) in BAL fluids from uninfected or BCG-infected mice.